Effects of Reinforcement Ratios and Sintering Temperatures on the Mechanical Properties of Titanium Nitride/Nickel Composites

Yi-Cheng Chen
National Kaohsiung University of Science and Technology https://orcid.org/0000-0002-6211-9109
Shih-Fu Ou (M9203510@gmail.com)
National Kaohsiung University of Science and Technology

Research Article

Keywords: Ti nitride, Ni, Metal-matrix composite, Carbothermal reduction reaction

Posted Date: June 30th, 2020

DOI: https://doi.org/10.21203/rs.3.rs-38133/v1

Version of Record: A version of this preprint was published at Materials on October 9th, 2020. See the published version at https://doi.org/10.3390/ma13204473.

Abstract

In this study, powder metallurgy was used to fabricate titanium nitride/nickel metal-matrix composites. First, Ti and Ni powders with weight ratios of 20:80, 50:50, and 80:20 were dry mixed for 24 h. After cold isostatic pressing, the green compacts were soaked in a water-based hot forging lubricant and sintered at 850, 950, and 1050°C for 1.5 h in an air atmosphere. The effects of the amount of titanium powder and the sintering temperature on the mechanical properties (hardness, wear resistance, and compressive strength) of the composites were investigated. The results indicated that titanium gradually transformed into titanium nitride near the surface after sintering due to the carbothermal reduction reaction; this transformation was observed to significantly increase the hardness. In addition, a titanium oxide film was observed to form between the titanium particles and the nickel matrix. The optimum sintering temperature of 950°C provides the composites with titanium-nickel weight ratios of 20:80 and 50:50, the latter of which exhibited the best mechanical properties (wear resistance and compressive strength). Furthermore, increasing the titanium content to 80% in the composite increased the hardness; however, the wear resistance and compressive strength were observed to reduce.

1. Introduction

Particle-reinforced metal matrix composites (PMMCs) are widely used in numerous applications such as in aviation, transportation, microelectronics, and nuclear industries; this is because of their excellent specific strength, thermal conductivity, and high-temperature as well as abrasion resistances [1–4].

PMMCs are reinforced by ceramic particles that have been dispersed in a metal matrix. Their excellent mechanical properties are attributed to (1) an external force load transfer between the matrix and the reinforcement, (2) dislocation strengthening, (3) refined grain strengthening, (4) precipitation hardening, (5) solid solution strengthening, (6) mixed strengthening, and (7) synergistic strengthening [5]. The four types of methods generally used to manufacture PMMCs are stir casting [6–9], pressure penetration [10], powder metallurgy [11–14], and mechanical alloying [10]. Although stir casting is a low-cost method that has been employed worldwide [2], powder metallurgy can avoid the following unwanted phenomenon, namely: (i) agglomeration of the ceramic particles during mechanical agitation, (ii) settling of the ceramic particulates, (iii) segregation of the secondary phases in the metal matrix, (iv) extensive interfacial reactions, and (v) ceramic particulate fracture during mechanical agitation [15].

Ceramic particles such as SiC, BN, TiC, TiB_2, TiN, ZrO_2, ZrN, MoC, WC, and Al_2O_3 are commonly used as metal matrix composite reinforcements [3, 10, 16]. However, ceramic powders with diameters of less than 50 μm (d_{50} < 50 μm) are cohesive because of the large interparticle force (electrostatic, Van der Waal's, and liquid bridge forces) [17]. Hence, achieving a uniform ceramic particle distribution in a metal matrix is challenging. Additionally, as the volume percentage of the reinforcing particles increases, agglomeration is more likely to occur [15]. This study used a carbothermal reduction reaction to transform metal particles into ceramic particles during sintering; this was aimed at overcoming the agglomeration of reinforcement particles.

Herein, two kinds of metal powders were mixed first, namely: titanium and nickel. The green compacts were soaked in a water-based hot forging lubricant and were sintered at elevated temperatures in an air atmosphere. The carbothermal reduction and diffusion reactions led to the formation of titanium nitride particles dispersed in the nickel matrix and simultaneously densified the green compacts. The effects of the sintering temperature and the reinforcement ratio on the microstructure and mechanical properties of the PMMCs were investigated. In addition, the interfacial adhesion between the metal matrix and the reinforcement particles was explored with wear tests.

2. Material And Methods

2.1. Sample preparation

Commercial Ti and Ni powders with average diameters of 75 and 45 μm, respectively, were used. Ti and Ni powders with three weight ratios of 20:80, 50:50, and 80:20 were dry mixed for 24 h by V-shaped mixer. The powder mixtures were consolidated into cylindrical compacts (φ10 × 15 mm) by cold pressing at 25 °C with a pressure of 637 MPa under atmospheric conditions by universal testing machine (SHIMADUZ, UH-1). After soaking the green ingots 30 seconds in a water-based hot forging lubricant which contained primarily C, N, and O, the green ingots were sintered at 850, 950, and 1050 °C for 1.5 h in air. The compacts with Ti/Ni weight ratios of 20:80, 50:50, and 80:20 were named T2N8, T5N5, and T8N2, respectively. The compacts with titanium/nickel and a weight ratio of 20:80 were sintered at 850℃, 950℃, and 1050℃ were named as T2N8-850, T2N8-950, and T2N8-1050, respectively.

2.2. Microstructural characterisation

The titanium nitride/nickel PMMC microstructures were characterised by high-resolution field emission scanning electron microscopy (SEM, JEOL JSM – 6330TF). The composition of the Ti nitride/Ni PMMCs was identified by an energy dispersive X-ray microanalyser (EDX, JEOL) equipped to the SEM. The crystalline structure of the Ti nitride/Ni PMMCs was assessed by an X-ray diffraction (XRD, SIEMENS D5000) analysis with Cu K_{α} radiation.

2.3. Mechanical properties tests

The porosity of the Ti nitride/Ni PMMCs was evaluated by the Archimedes' technique. The microhardness of the composites was measured by Vickers indentations (Micro-Vickers Hardness Meter–Mitutoyo_MVK–H1). Indentations were made on a perpendicular polished surface using a load of 50 g. The indentations were then examined by an optical microscope (OLYMPUS). Additionally, the HRA hardness of the composite material was measured at three different locations on the surface using a Rockwell hardness tester and load of 60 kgf (Akashi Corporation AR-10). The wear test was performed with a ball-on-disk wear tester (SENSE). Dry grinding processes with a 1 kg load and 200 rpm rotation speed were performed on the surface of the sample at 22, 44, 66, 88, and 110 m, respectively. After the abrasion stopped, the weight of the specimen was measured for weight loss. The compressive strength test was examined by a universal tester (JANOME JP-5004), and the compression rate was 1 mm/min.

3. Results And Discussion

3.1 PMMC microstructure

Figure 1 and Table 1 show the morphology and composition of T8N2-850, respectively. Figure 1 shows the nickel matrix (site a), the titanium particle (site e), and the interface layer (site c). The interface layer—with a high concentration of oxygen and titanium was named Ti-oxide-film. Parts of the Ti-oxide were dispersed in the matrix, as shown in site b. The layer (site d) with a thickness of about 3 μm and a high content of titanium, oxygen, and nitrogen was named the Ti-nitride-layer.

The boundary of the titanium particle (site d) in Figure 1 shows that oxidation and nitridation reactions occur on the titanium particles in a high-temperature sintering process under atmospheric conditions. The free energy of the titanium and oxygen reaction is lower than that of the titanium and nitrogen reaction [18]; therefore, the oxidation reaction takes precedence over the nitridation reaction on the titanium surface. However, the hot forging lubricant covering the titanium particles helped prevent the titanium from making contact with the oxygen. Additionally, the carbon content decreased significantly in the Ti-nitride-layer according to the following carbothermal reduction reaction:

$$2TiO_2 + 4C + N_2 \rightarrow 2TiN + 4CO\uparrow \quad (1)$$

The carbothermal reduction reaction converts a portion of the titanium oxide to titanium nitride. Simultaneously, the carbon monoxide gas released from the interface breaks the titanium oxide layer. Consequently, the Ti-oxide-film fragments are dispersed into the matrix around the titanium particles as shown at site b in Figure 1.

In order to investigate the effect of temperature on the carbothermal reduction reaction, the thickness of the Ti-nitride-layer, the titanium particles, and the Ti-oxide-film covering the outer surface of the titanium particles were measured by SEM. The average thickness—shown in Figure 2—was calculated by measuring at least seven sites. The thickness of the Ti-nitride-layer increased as the sintering temperature increased (Figure 2(a)). In addition, the thickness of the Ti-oxide-layer depends not only on the temperature but also on the proportion of titanium in the PMMC (Figure 2(b)). Before sintering, the PMMC ingot will be soaked in the CONDAT solution. The solution with C and O elements can penetrate into the interior of the PMMC through the gaps between the powders. Compared with T5N5 and T8N2, T2N8 has the smallest numbers of Ti particles. For T2N8, each Ti particle obtains relatively higher amounts of CONDAT solution to cover the surface when comparing with T5N5 and T8N2; therefore, T2N8 has a thickest oxide layer during sintering at 1050℃.

Figure 3 shows the SEM micrograph of T2N5, T5N5, and T8N2 sintered at 850, 950, and 1050 ℃, respectively. The T2N8-850 titanium particles were easily detached from the nickel matrix by specimen polishing as indicated by the arrow in Figure 3(a). Most of the T2N8-950 titanium particles remained in the nickel matrix because of the thick Ti-oxide-film that bound the particles and the matrix. However, some pores appeared in the Ti-nitride-layer of the titanium particles as shown in Figure 3(b). In Figure

3(c), the titanium particles remained in the nickel matrix, but fractures were observed within the titanium particles, indicating that Ti-oxide-film bonds well with the nickel matrix, but that the numerous defects in the titanium particles fracture the titanium particles when the specimen is polished. Figure 3(d–f) shows a similar situation for the T5N5 sintered at 850, 950, and 1050 ℃, respectively.

For T8N2-850 (Figure 3(g)), the detachment of the titanium particles is more frequent than for T2N8-850, and parts of the titanium particles inter-diffuse with each other in T8N2 sintered at 950 and 1050 ℃, as shown in Figure 3(h–i), respectively. The detachment of the nickel matrix was observed in Figure 3(i) after polishing, as titanium is harder than the nickel.

3.2 PMMC composition

Figures 4–6 show XRD spectra of the T2N8, T5N5, and T8N2 compacts sintered at 850, 950, and 1050 ℃, respectively. As shown in Figure 4, the Ni phase in the XRD pattern of T2N8-850 is the main phase, and the intensity of the $TiN_{0.3}$ diffraction peak is very weak. As the sintering temperature was further increased to 950 ℃, the intensity of the $TiN_{0.3}$ diffraction peak decreased, and the TiN diffraction peak appeared. When the sintering temperature reached 1050 ℃, the intensity of the diffraction peaks of both TiN and TiO_2 significantly increased. A SEM-EDS analysis showed that titanium oxide was formed at 850 ℃. However, the titanium content of T2N8 is low, and the titanium oxide forms only on the outer surface of the titanium particles, which results in low titanium oxide content. Therefore, titanium oxide cannot be detected in the XRD pattern of T2N8-850.

The XRD spectra of T5N5 in Figure 5 show why $TiN_{0.3}$ was formed at 850 ℃. At 950 ℃, titanium is transformed into TiO_2 and TiN. As the sintering temperature increased to 1050 ℃, the diffraction peaks of TiN increased, while the diffraction peak of TiO_2 decreased, suggesting that the thickness of the titanium nitride layer increases with sintering temperature because of violent carbothermal reduction reactions at 1050 ℃.

Figure 6 shows that the diffraction peaks of the TiO_2 and TiN phases appear at 850, 950, and 1050 ℃. Additionally, the intensity of the titanium oxide and nitride peaks of T8N2 is higher than that of T2N8 and T5N5. As the sintering temperature increased from 950 to 1050 ℃, $I_{TiN(200)}/I_{TiO2(111)}$ also increased. Thus, the thickness of the Ti-oxide-film first increases with sintering temperature up to 950 ℃ and then decreases, as measured by SEM observation (Figure 2). The intensity of TiN0.3 and TiN peaks increase significantly with the weight percentage of Ti in MMC under various sintering temperature.

3.3 PMMC porosity

Table 2 shows the porosity of pure nickel, T2N8, T5N5, and T8N2. As the sintering temperature increased from 850 to 950 ℃, the porosity of the pure nickel decreased from 9.02% to 2.01%. The porosity of T2N8-950 is lower than that of T2N8-850 because the pores are eliminated by the thermal diffusion of the nickel powders. However, the carbothermal reduction reaction occurs violently at high temperatures (1050 ℃) and forms numerous pores. Hence, the porosity of T2N8 increased to 10.43% when the T2N8

compact was sintered at 1050 ℃. The porosity of the sintered T5N5 and T8N2 compacts increased with increased sintering temperature, indicating that the degree of pore formation is greater than that of compact shrinkage from diffusion. This is because the high titanium content in the compacts fuels the carbothermal reduction reaction, which produces numerous pores.

The porosity of T5N5 is lower than that of T2N8 and T8N2 sintered at 850, 950, and 1050 ℃. According to the literature, a wider powder particle distribution range, stable sintered compact shrinkage rate, and smaller pores produce a more uniform crystal phase distribution [19]. In this study, the average particle sizes of titanium and nickel powders are 75 and 45 μm, respectively. When the weight ratio of these two powders is equivalent, a larger particle size distribution range is obtained; therefore, the porosity of Ti5N5 is lower than that of T2N8 or T8N2.

3.4 PMMC hardness

Figure 7(a) shows the Rockwell hardness of T2N8, T5N5, and T8N2 sintered at 850, 950, and 1050 ℃. The hardness increased with an increased sintering temperature and number of titanium particles. Figure 7(b) shows the hardness of the centre of the T2N8 titanium particle as measured by the Vickers microhardness tester. The hardness of the PMMC is greater than that of than pure titanium (150 HV) and nickel (123.6 HV) [20,21]. The transformation of titanium into TiN and $TiN_{0.3}$ reinforces the PMMC and increases the amount of titanium particles.

Figure 8 shows the indentation location of the Vicker's microhardness of T2N8-950 observed by an optical microscope. The centre of the titanium particle is HV1033.0 in Figure 8(a). The hardness of the Ti-oxide-film is HV318.2, which is between that of the nickel matrix (HV79.7) and the titanium particles (HV1033.0) in Figure 8(b).

3.5 PMMC wear resistance

The factors affecting the wear resistance of a composite include (1) the number of reinforcing materials in the matrix, (2) the combination of reinforcing materials in the matrix, and (3) the porosity of the composite. In Figure 9(a), T2N8 sintered at 850 and 950 ℃ has the highest and lowest weight loss, respectively. The thickness of the Ti-oxide-film makes strengthen the bonds between the reinforcing material and the matrix. However, the porosity generated by the carbothermal reduction reaction increases rapidly at 1050 ℃ and lowers the wear resistance of T2N8-1050 more than that of T2N8-950. T2N8-850 has the lowest wear resistance because the thickness of its Ti-oxide film is very small. T2N8-850 has the lowest hardness among the T2N8 compacts. T5N5 shows the same relationship between wear resistance and sintering temperature as does T2N8 (Figure 9(b)).

Figure 9(c) shows the wear resistance of T8N2 sintered at 850, 950, and 1050 ℃. T8N2-1050 and T8N2-850 have the lowest and highest weight loss, respectively. The T8N2 matrix consists primarily of titanium particles, some of which with each other. Therefore, the bonding ability of titanium particles increased with the sintering temperature, leading to a significant reduction in weight loss. However, since the nickel

content is low, the nickel powder is discontinuously distributed in the titanium matrix; therefore the nickel peels off easily, as shown in Figure 3. Furthermore, multiple carbothermal reduction reactions cause poor interfacial adhesion between the titanium and the nickel and allow titanium particles to be easily worn away. Hence, the T8N2 compacts have the lowest wear resistance among the sintered compacts.

T8N2 has the highest hardness but the lowest wear resistance of the sintered compacts. Previous studies found that the hardness and the wear resistance of composites are not directly related. During wear processing, shear stress occurs on the PMMC, and cracks may appear in the matrix [22]. As a result, even if the hardness of the PMMC is enhanced by particle reinforcement, the PMMC may be easily peeled off from internal cracks.

3.6 PMMC compressive strength

Figure 10(a–c) show the compressive stress-strain curves of T2N8, T5N5, and T8N2 sintered at 850, 950, and 1050 ℃, respectively. A sintering temperature of 950 °C provides a higher compressive strength for T2N8 and T5N5 than does 1050 ℃ (a–b). The worse compressive strength is from the high porosity of the compacts sintered at 1050 °C. The position around the pores is likely to cause stress concentration and become the starting point of deformation. The compressive strength of T2N8 and T5N5 sintered at 1050 °C is higher than that of T2N8 and T5N5 sintered at 850 °C. This result is consistent with the wear test. Furthermore, T8N2 exhibited the lowest compressive strength of the sintered compacts (Figure 10(c)), because T8N2 has high amounts of hard material (titanium) and low amounts of soft material (nickel). This combination produces brittle fractures when the compacts are under compressive loads.

4. Conclusion

This study successfully fabricated a titanium nitride/nickel composite through the carbothermal reduction reaction, which was achieved by sintering the compacts of titanium and nickel that were mixed with a hot forging lubricant. The effects of the titanium powder ratios (20, 50, and 80 wt%) and sintering temperatures (850, 950, and 1050 ℃) on the mechanical properties of the PMMC were investigated. The PMMCs with titanium-nickel weight ratios of 20:80 and 50:50 sintered at 950 ℃ exhibited the highest wear resistance and compressive strength among other groups. A titanium-oxide-film was observed to form around the titanium nitride and provided good bonding with the nickel matrix. A violent carbothermal reduction reaction was induced at high temperatures (1050 ℃) and generates abundant pores in the PMMC, which deteriorate the wear resistance and the compressive strength.

References

[1] Singla M, Dwivedi DD, Singh L, et al. Development of aluminium based silicon carbide particulate metal matrix composite. J Min Mater Charact Eng 2009, 8: 455–467.

[2] Behera R, Chatterjee D, Sutradhar G. Effect of reinforcement particles on the fluidity and solidification behavior of the stir cast aluminum alloy metal matrix composites. Am J Mater Sci 2012, 2: 53–61.

[3] Godfrey TMT, Goodwin PS, Ward-Close CM. Titanium particulate metal matrix composites reinforcement, production methods, and mechanical properties. Adv Eng Mater 2000, 2: 85–92.

[4] Kainer KU, Geesthacht HZ. Basics of Metal Matrix Composites. Weinheim (DE): Wiley-VCH Verlag GmbH & Co KGaA, 2006.

[5] Chen J, Wu G, Sun D, et al. Strengthening mechanism of metal matrix composites. J Aeronaut Mater 2002, 22: 49–53.

[6] Wang SY, Tang Q, Li DJ, et al. The hot workability of SiCp/2024 Al composite by stir casting. Mater Manuf Process 2015, 30: 624–630.

[7] Syahrial AZ, Pancasakti A. Effect of aging on characterization of sr-modified stir cast A356/Al_2O_3 composite. Key Eng Mater 2017, 753: 33–38.

[8] Viswanatha BM, Prasanna Kumar M, Basavarajappa S, et al. Study the formation of mechanically mixed layer and subsurface behavior of worn out surfaces of aged hybrid metal matrix composites. Ind Lubr Tribol 2018, 70: 818–827.

[9] Singh B, Kumar J, Kumar S. Investigation of the tool wear rate in tungsten powder-mixed electric discharge machining of AA6061/10%SiCp composite. Mater Manuf Process 2016, 31: 456–466.

[10] Bajakke PA, Malik VR, Deshpande AS. Particulate metal matrix composites and their fabrication via friction stir processing – a review. Mater Manuf Process 2019, 34: 1–49.

[11] Casati R, Vedani M, Dellasega D, et al. Consolidated Al/Al_2O_3 nanocomposites by equal channel angular pressing and hot extrusion. Mater Manuf Process 2015, 30: 1218–1222.

[12] Soltani N, Sadrnezhaad SK, Bahrami A. Manufacturing wear-resistant 10Ce-TZP/Al_2O_3 nanoparticle aluminum composite by powder metallurgy processing. Mater Manuf Process 2014, 29: 1237–1244.

[13] Lakshmipathy J, Rajesh Kannan S, Manisekar K, et al. Effect of reinforcement and tribological behaviour of AA7068 hybrid composites manufactured through powder metallurgy techniques. Appl Mech Mater 2017, 867: 19–28.

[14] Khosla P, Singh HK, Katoch V, et al. Synthesis, Mechanical and corrosion behaviour of iron–silicon carbide metal matrix nanocomposites. J Compos Mater 2018, 52: 91–107.

[15] Srivatsan TS, Ibrahim IA, Mohamed FA, et al. Processing techniques for particulate-reinforced metal aluminium matrix composites. J Mater Sci 1991, 26: 5965–5978.

[16] Stefanescu DM. Issues in liquid processing of particulate metal matrix composites. Key Eng 1993, 79-80: 75–90.

[17] Mazurnder MK, Mountain JR. Fluidity and flow properties of fine powders. Particul Sci Technol 1997, 15: 106.

[18] Wicks CE, Block FE. Thermodynamic properties of 65 elements-their oxides, halides, carbides, and nitrides. Washington (US): United States Government Printing Office, 1963.

[19] Ting JM, Lin RY. Effect of particle-size distribution on sintering Part I Modelling. J Mater Sci 1994, 29: 1867–1872.

[20] Hacisalihoglu I, Samancioglu A, Yildiz F, et al. Tribocorrosion properties of different type titanium alloys in simulated body fluid. Wear 2015, 332-333: 679–686.

[21] Anand TJS. Nickel as an alternative automotive body materials. J Mech 2012, 2: 187–197.

[22] Zhang ZF, Zhang LC, Mai YW. Wear of ceramic particle-reinforced metal-matrix composites. J Mater Sci 1995, 30: 1967–1971.

Tables

Table 1: Chemical composition of T8N2-850 detected by EDS. The detected areas a, b, c, d, and e, are marked in Figure. 1

Element (at%)	a	b	c	d	e
C	8.2	1.7	4.2	0.7	5.1
N	0	0	0	28.4	5.9
O	7.5	72.0	67.3	27.9	31.7
Ti	2.7	25.0	25.5	42.9	57.3
Ni	81.6	1.3	3.0	0.1	0

Table 2: Porosity and density of pure nickel, T2N8, T5N5, and T8N2 sintered at various temperatures

Porosity				
	Pure Ni	T2N8	T5N5	T8N2
850°C	9.02%	9.47%	6.71%	7.39%
950°C	2.01%	7.72%	6.88%	7.81%
1050°C	4.32%	10.43%	8.10%	9.74%
Density (g/cm^3)				
	Pure Ni	T2N8	T5N5	T8N2
850°C	8.10	7.27	6.26	4.99
950°C	8.73	7.41	6.25	4.97
1050°C	8.52	7.19	6.16	4.86

Figures

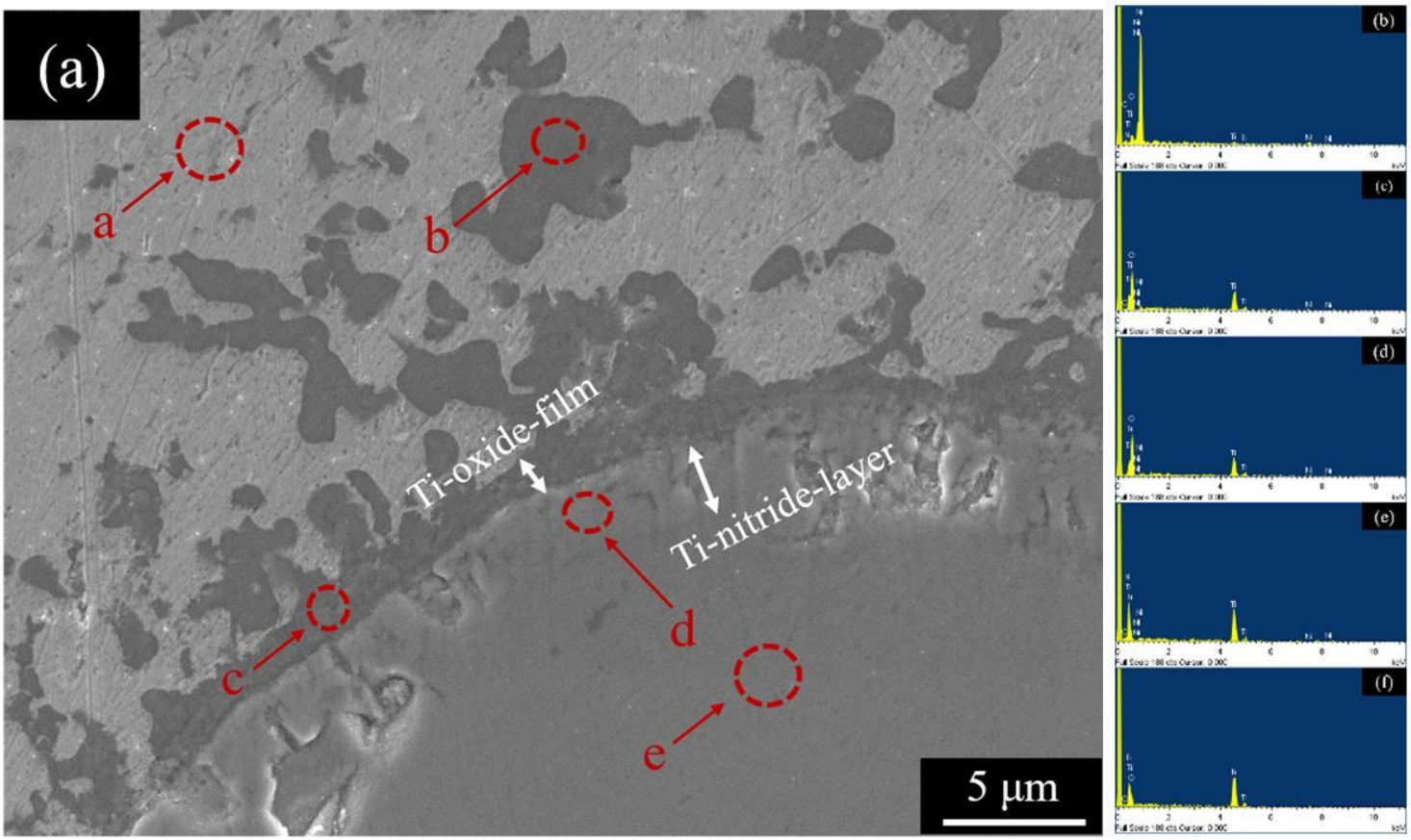

Figure 1

(a) SEM micrograph of T8N2-850, (b) EDS spectrum of site a, (c) EDS spectrum of site b, (d) EDS spectrum of site c, (e) EDS spectrum of site d, (f) EDS spectrum of site e.

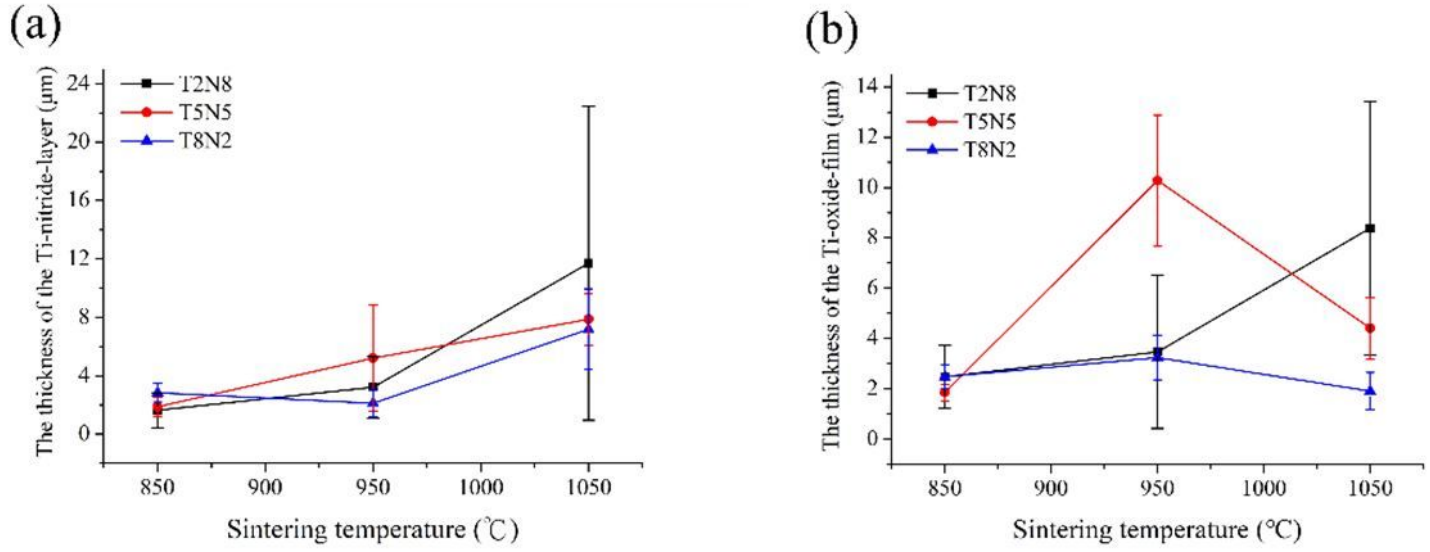

Figure 2

(a) Thickness of the Ti-nitride-layer of the titanium particle. (b) Thickness of the Ti-oxide-film between the titanium particle and the nickel matrix.

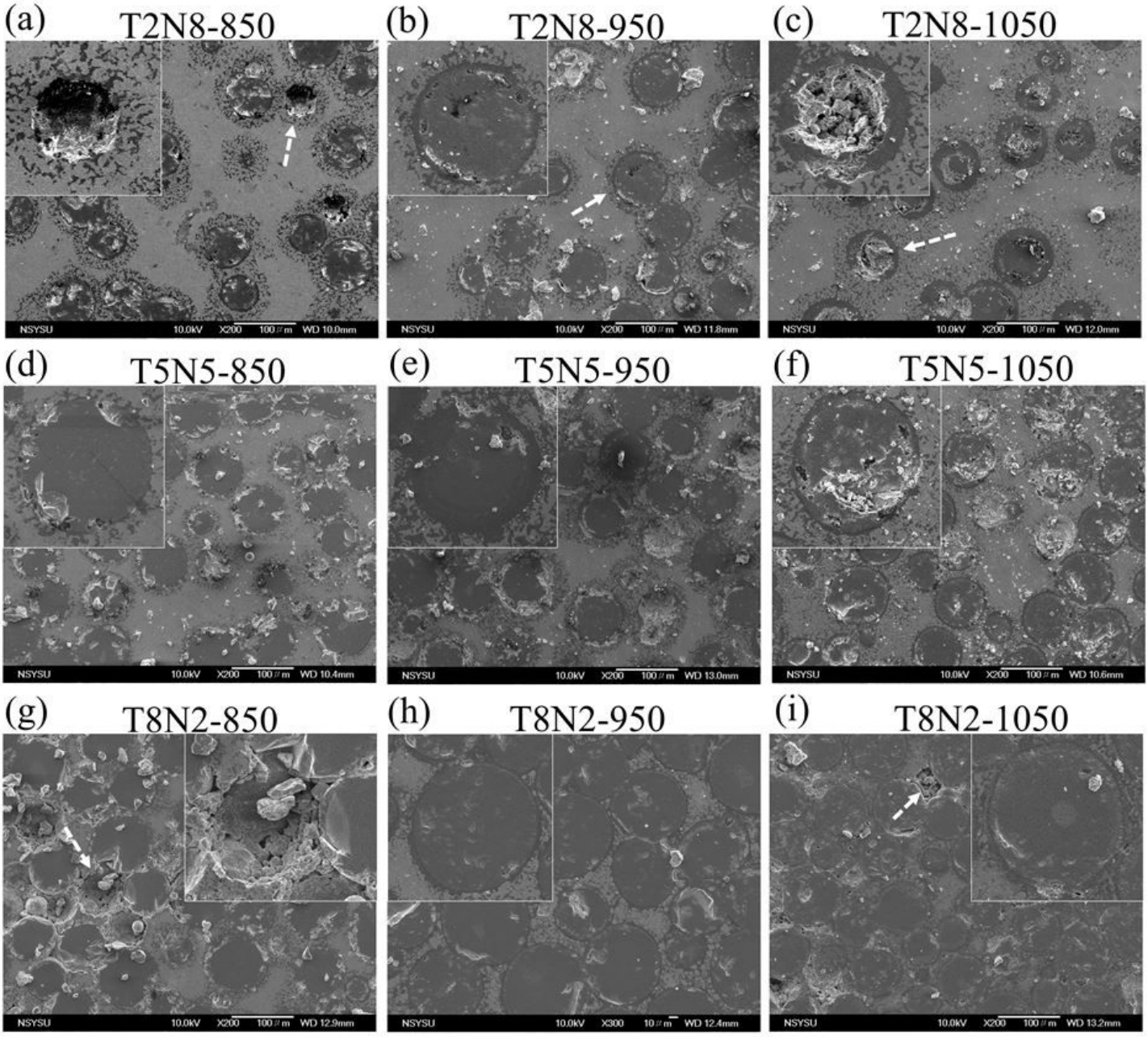

Figure 3

SEM micrograph of T2N5, T5N5, and T8N2 sintered at 850, 950, and 1050 °C. (a) T2N8-850, (b) T2N8-950, (c) T2N8-1050, (d) T5N5-850, (e) T5N5-950, (f) T5N5-1050, (g) T8N2-850, (h) T8N2-950, and (i) T8N2-1050.

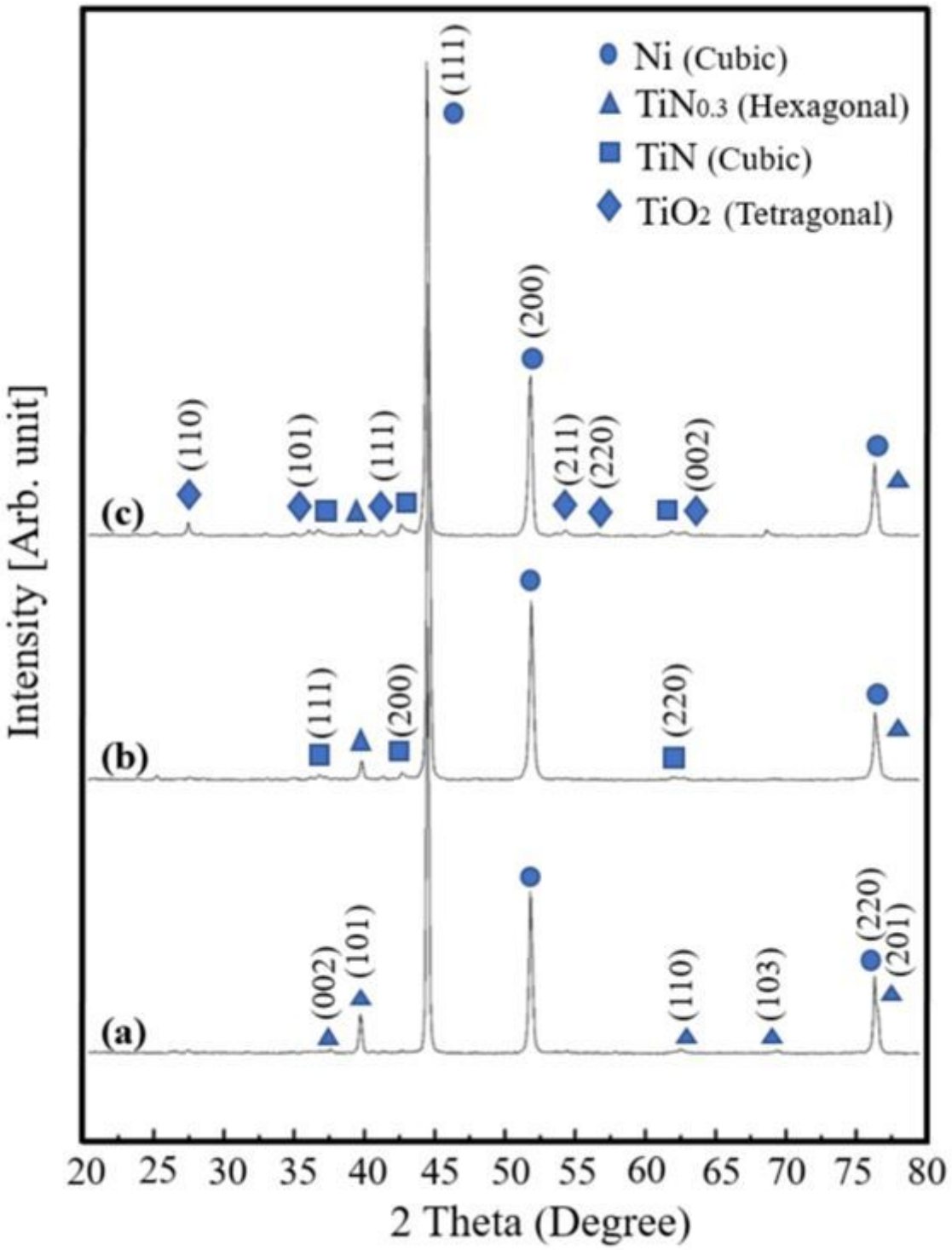

Figure 4

XRD spectra of the T2N8 compact sintered at (a) 850, (b) 950, and (c) 1050 °C.

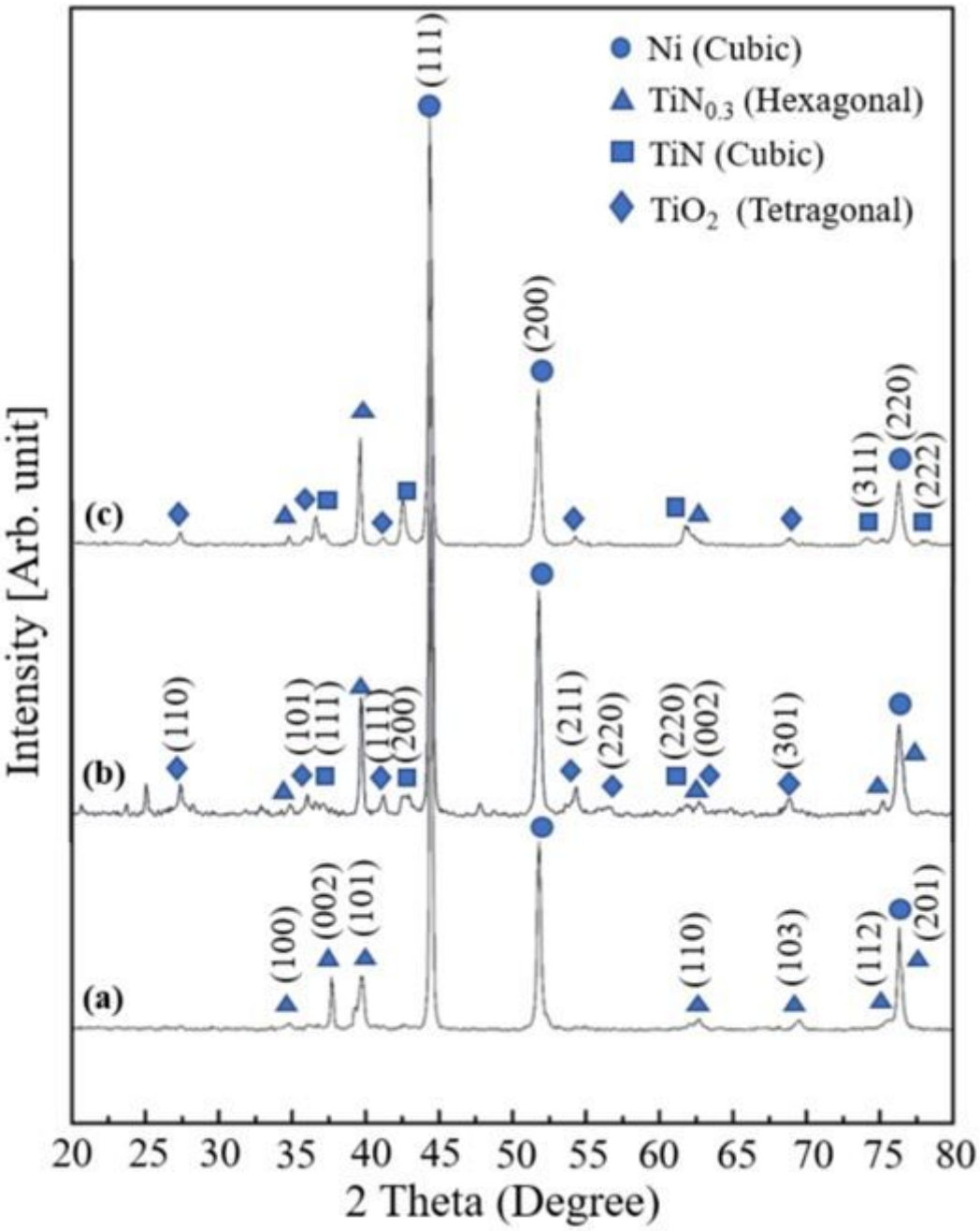

Figure 5

XRD spectra of the T5N5 compact sintered at (a) 850, (b) 950, and (c) 1050 °C.

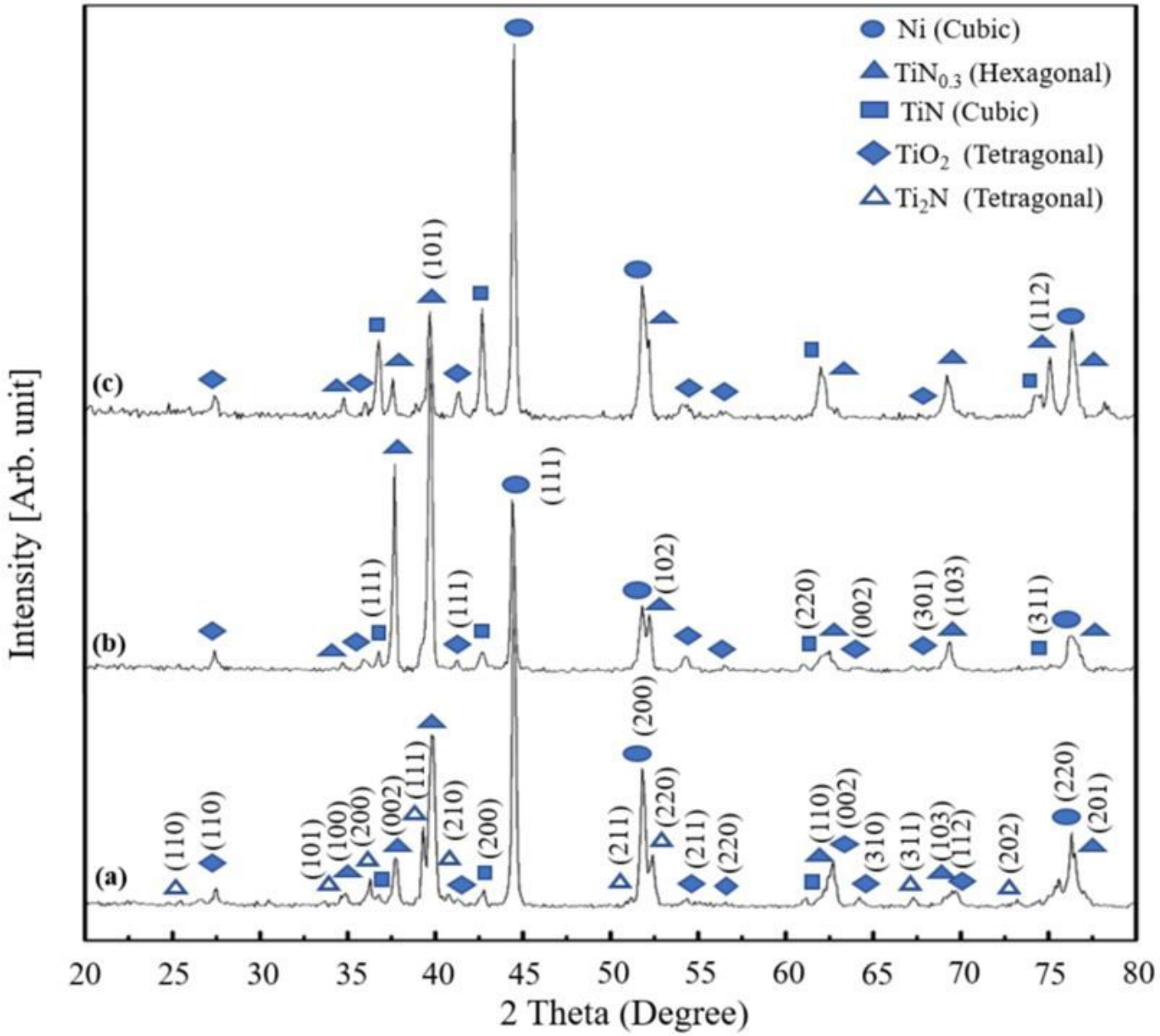

Figure 6

XRD spectra of the T8N2 compact sintered at (a) 850, (b) 950, and (c) 1050 °C

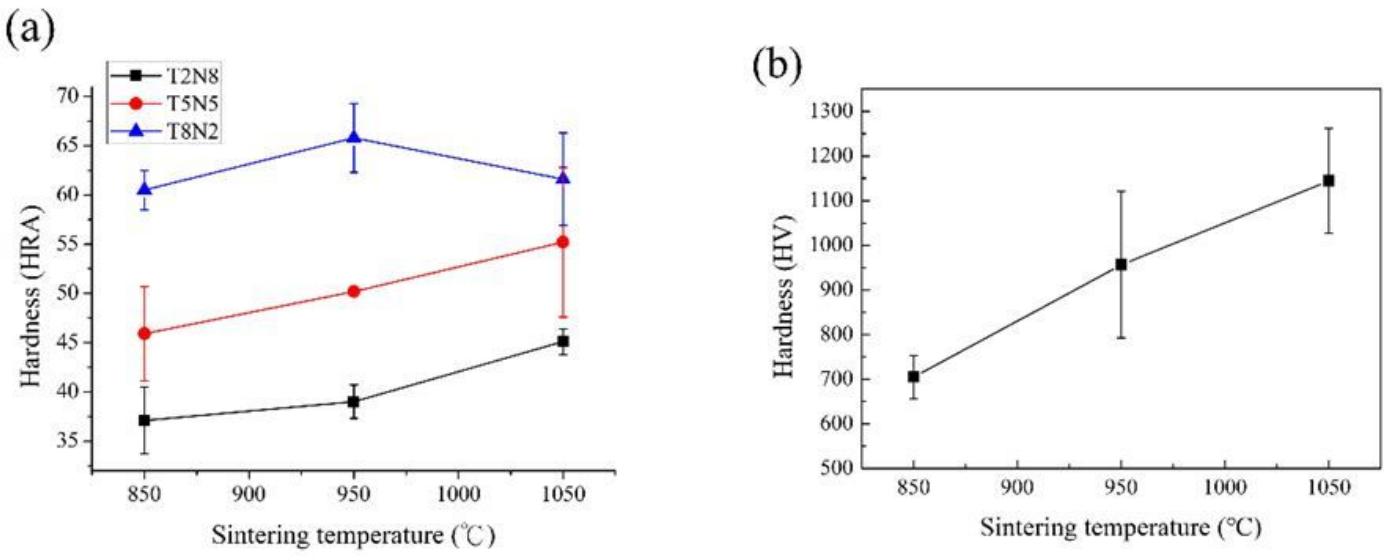

Figure 7

(a) Rockwell hardness of T2N8, T5N5, and T8N2 sintered at 850, 950, and 1050 ℃. (b) Vickers microhardness of T2N8. Indentation is at the centre of the titanium particle sintered at 850, 950, and 1050 ℃.

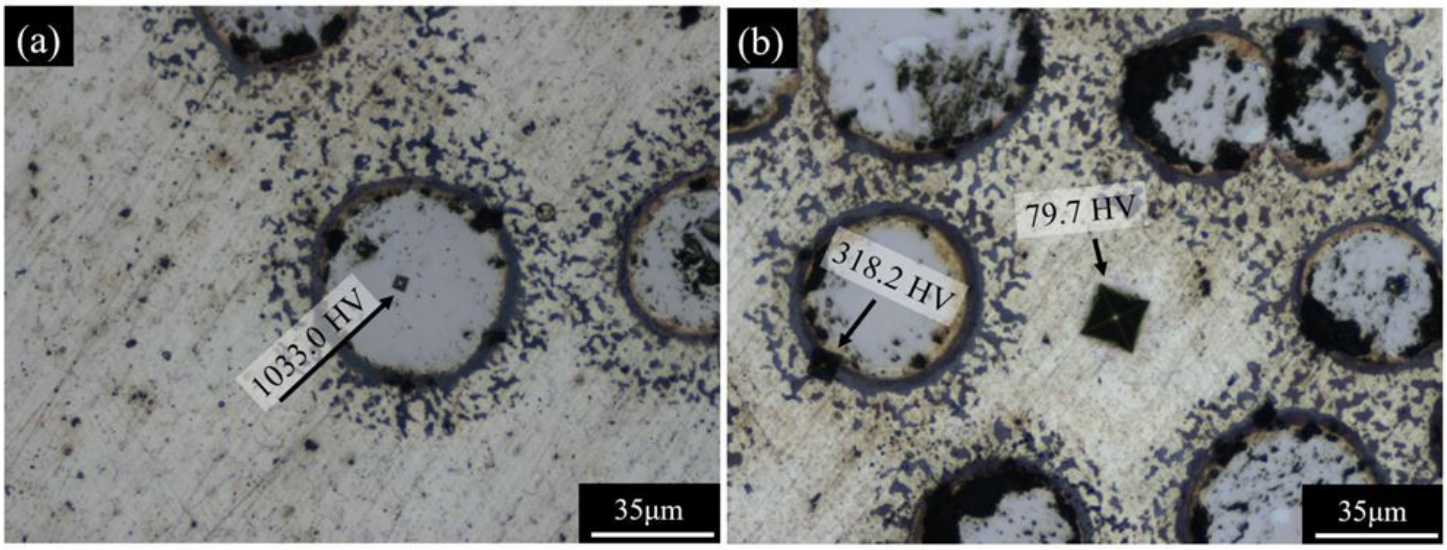

Figure 8

(a) OM image of the indentation location in centre of the T2N8-950 titanium particles. (b) OM image of the indentation location in the T2N8-950 nickel matrix and Ti-oxide-film.

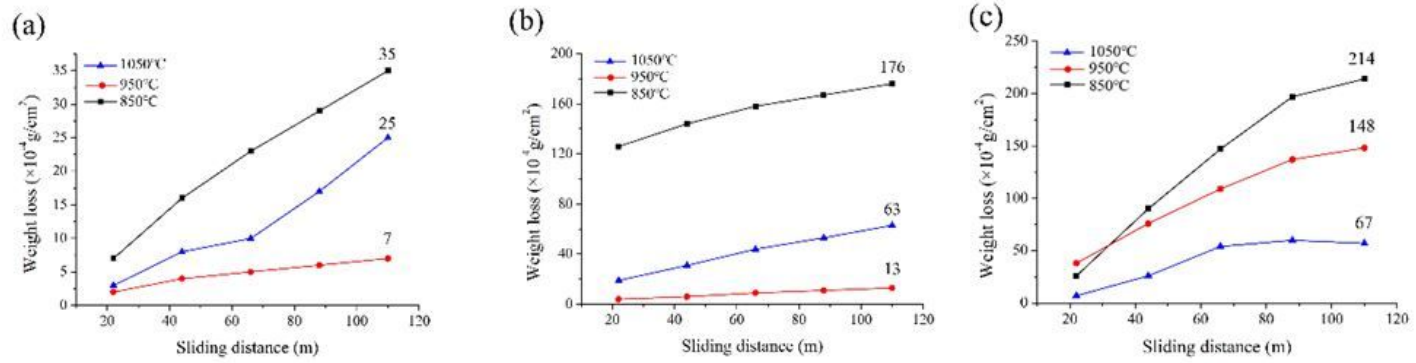

Figure 9

Weight losses of (a) T2N8, (b) T5N5, and (c) T8N2 sintered at 850, 950, and 1050 °C after wear tests.

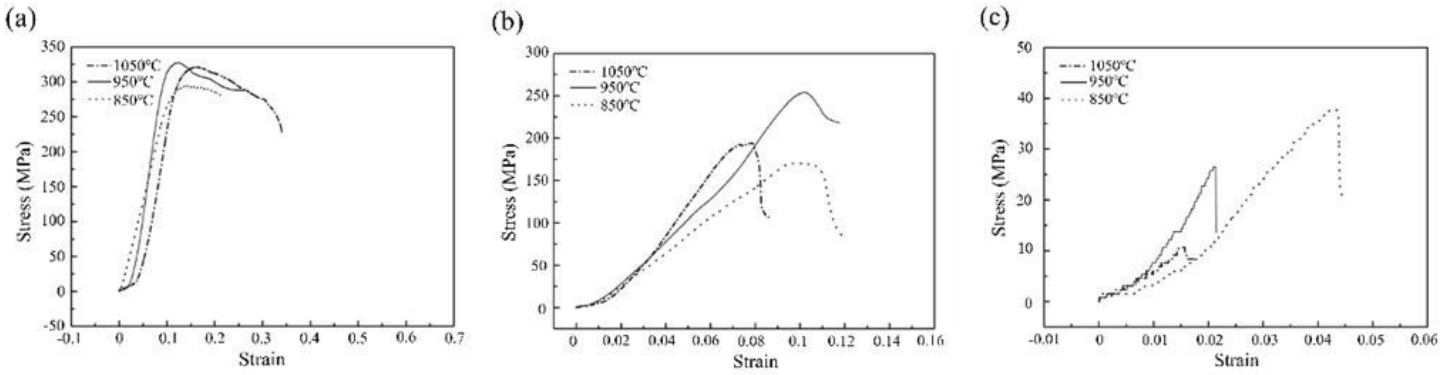

Figure 10

Stress-strain curves of (a) T2N8, (b) T5N5, and (c) T8N2 sintered at 850, 950, and 1050 °C under compressive tests.

Supplementary Files

This is a list of supplementary files associated with this preprint. Click to download.

- declaration.docx
- declaration.docx
- Coverletter.docx
- Coverletter.docx